# Communication

## A Broadband and High-Gain Endfire Antenna Array Fed by Air-Substrate Parallel Strip Line

Yuefeng Hou, Yue Li, Zhijun Zhang, and Zhenghe Feng

***Abstract*— A broadband and high-gain endfire antenna array fed by an air-substrate parallel strip line is proposed in this communication. It has a simple and planar structure consisting of multiple dipole radiating elements and one parallel strip line. By utilizing the center-fed dipole working between the first and third resonances as the radiating element, the antenna array could obtain stable radiating capability over a broad bandwidth. Fed by an air-substrate parallel strip line working on the TEM mode, the antenna array achieves a moderate phase constant, which is helpful for realizing stable endfire radiation. The radiating element separation is optimized to eliminate the high-order spatial harmonics, ensuring single beam radiation. Fabricated by thin copper plates, the merits of the antenna array include lightweight, low cost, and easy fabrication. According to the measured results, the antenna array has a good match and a stable endfire radiation pattern over the operating band from 4 to 10.5 GHz with the measured gain varying from 10.1 to 13.5 dBi.**

***Index Terms*— Air-substrate, all metal, broadband, endfire antenna, high gain, parallel strip line, planar.**

### I. Introduction

Planar endfire antennas with wideband and high gain have been investigated frequently in response to the growing requirements of broadband long distance wireless applications. The Yagi-Uda antenna is a classic high-gain endfire antenna. It has been the subject of exhaustive analytical and experimental studies in the open literature [1]–[4]. The typical geometry of the Yagi-Uda antenna is depicted in Fig. 1(a), which consists of a number of directors, a driver element, and a reflector [5]. To enlarge the impedance bandwidth, it is essential to adopt a wideband transition structure to excite the driver element [6]–[10]. A multi-resonant [6] or self-complementary driver element [7] would be good for a lager operating bandwidth. By optimizing the configuration of the reflector [8], [9], the unidirectional radiation characteristics are improved over a broad frequency band. Although wide bandwidths were achieved by the antennas in [6]–[10], the numbers of the parasitic directors are small, which leads to a somewhat low gain.

The most recognized structure of the log-periodic antenna [5] is illustrated in Fig. 1(b). It consists of one feed line and a sequence of side-by-side radiating elements with certain-growth-rate lengths along the radiating aperture. As the frequency increases, the role of active elements passes from the longer to the shorter elements [11]–[15], realizing a broad impedance match property. As a result, it is observed that partial radiating aperture is used at each frequency point.

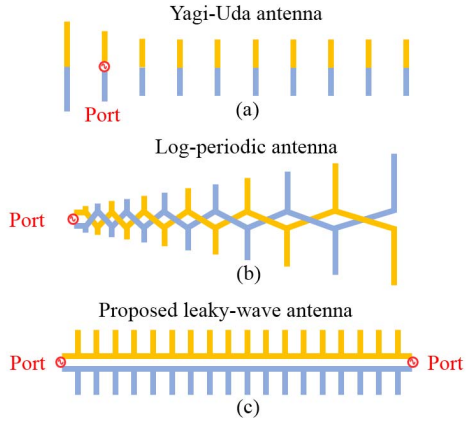


Fig. 1. Geometries of (a) typical Yagi-Uda antenna, (b) typical log-periodic antenna, and (c) proposed antenna array.

To increase the gain, the antenna with clamped mode was demonstrated in [16], which enlarges the width of the radiating aperture. By adding several parasitic directors on the front of the log-periodic antenna, the radiating aperture length could be expanded to improve the gain [17], [18]. Nevertheless, the antennas in [16]–[18] are with a relatively short radiating aperture, which restricts the maximum range of the gain.

Hence, although much research effort has been made, it is still a challenge to design a high-gain endfire antenna over a wide bandwidth, owing to the limitation of the radiating aperture length.

In recent years, leaky-wave antennas with large radiating aperture length fed by substrate integrated waveguide (SIW) [19], [20] or air-substrate microstrip line [21]–[24] have sparked considerable interest. With a small coupling level between the radiating elements and feeding structure, they could readily obtain an approximately uniform magnitude distribution, which is suitable for the realization of high gain. Nevertheless, since the operating mode in the SIW of the antennas in [19] and [20] is the dispersive $TE_{10}$ mode, the main beam direction varies drastically versus frequency. Although the antennas in [21]–[24] works on a nondispersive TEM mode, the main beam direction deviates from the endfire direction due to the limited ground plane and because the operating bandwidths are relatively narrow due to the unstable coupling level of the radiating elements.

Inspired by the works in [19]–[24], in this communication, we propose a novel endfire antenna array fed by an air-substrate parallel strip line. The simplified geometry of the proposed antenna array is distinctly different from the Yagi-Uda antenna or log-periodic antenna, as plotted in Fig. 1(c). Fed by the parallel strip line, the antenna array could be designed with a large radiating aperture length to enlarge the gain. Working on the TEM mode, the air-substrate parallel strip line provides a moderate phase velocity

Manuscript received March 5, 2019; revised May 6, 2019; accepted May 27, 2019. Date of publication June 6, 2019; date of current version August 12, 2019. This work was supported by the National Natural Science Foundation of China under Contract 61525104. *(Corresponding author: Zhijun Zhang.)*

The authors are with the Department of Electronic Engineering, Beijing National Research Center for Information Science and Technology (BNRist), Tsinghua University, Beijing 100084, China (e-mail: zjzh@tsinghua.edu.cn).

Color versions of one or more of the figures in this communication are available online at http://ieeexplore.ieee.org.

Digital Object Identifier 10.1109/TAP.2019.2920332

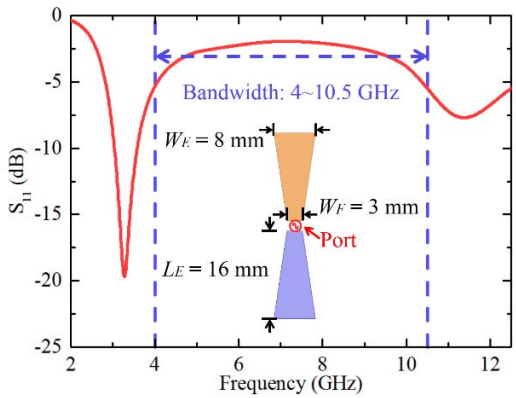


Fig. 2. Geometry and reflection magnitude of the radiating element.

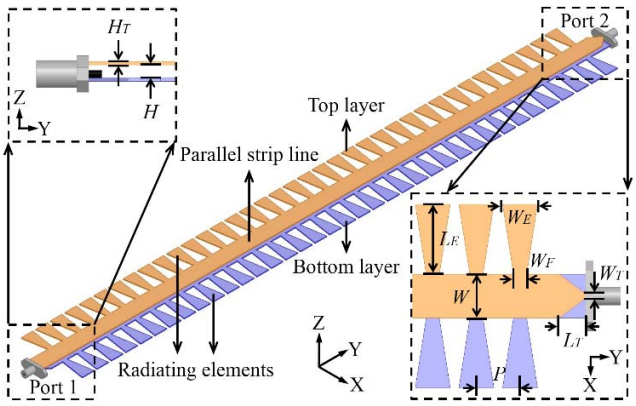


Fig. 3. Geometry of the antenna array.

for endfire radiation. With a dense arrangement of the radiating elements, high-order spatial harmonics are restrained to ensure the single beam radiation. By adopting multiple identical radiating elements with stable and suitable coupling level, the radiating aperture has an almost equal magnitude distribution over a broad bandwidth. Consequently, the proposed antenna array achieves the properties of broadband, high-gain, and stable radiation pattern. In Section II, the design considerations, operating principles, and performance analyses are systematically investigated. In Section III, a prototype is fabricated and measured to verify the design strategy.

## II. Design and Analysis

### A. Geometry of the Antenna Array

The geometry and the reflection magnitude of a bowtie-shaped dipole antenna are illustrated in Fig. 2. When excited at the center, the first (around 3.3 GHz) and third (around 11.4 GHz) resonances of the dipole antenna are well matched, whereas the second resonance is not energized effectively. Between the first and third resonances, the dipole antenna has a high input impedance. A high-impedance radiating element only couples a small amount of energy from the parallel strip line and allows most energy traveling along, which is the desired merit for the radiating elements design in the leaky-wave antenna [25], [26]. As shown in Fig. 2, the reflection magnitude of the dipole antenna is relatively stable with an average value of −2.7 dB over the bandwidth from 4 to 10.5 GHz. Thus, the proposed dipole antenna working between the first and third resonances is adopted in the antenna array as the radiating element.

The antenna array consists of 37 identical radiating elements and an air-substrate parallel strip line, as plotted in Fig. 3. It has a planar and simple structure, which could be fabricated by thin metallic plates. Two SMA connectors are added on the two ends of the parallel strip line as the feed ports. To reduce the effect of the discontinuities between the parallel strip line and SMA connectors, tapered structures are applied. As shown in Fig. 3, all of the identical radiating elements are arranged in a line. The radiating elements are center-fed, and arms of each element are connected to corresponding parallel strip lines. The dimensions of the antenna array are given in Table I in detail.

### B. Design Procedure

The design of the proposed antenna could be separated into two independent parts: 1) optimizing the dimension of the radiating elements and 2) matching the parallel strip line

TABLE I
Dimension of the Antenna Array

| Parameter | Values (mm) | Parameter | Values (mm) |
|---|---|---|---|
| $L_T$ | 6 | $W$ | 10 |
| $L_E$ | 16 | $W_T$ | 1 |
| $H$ | 2 | $W_E$ | 8 |
| $H_T$ | 0.5 | $W_F$ | 3 |
| $P$ | 10 | | |

$$(AF)_N = \frac{1}{N}\left[\frac{\sin\left(-\frac{N}{2}kP\sin\theta + kP\right)}{\sin\left(-\frac{1}{2}kP\sin\theta + kP\right)}\right] \quad (1)$$

$$\sin(\theta_n) \cong \frac{\beta_n}{k_0} = \frac{\beta_0}{k_0} - \frac{2n\pi}{k_0 P}. \quad (2)$$

From Fig. 4, it is noted that increasing the length $L_E$ and width $W_E$ could both make the frequency response of the radiating element shift to a lower frequency band. Therefore, the radiating element with a larger width $W_E$ is preferred by the antenna array, because it has a smaller length $L_E$, which could miniaturize the dimension of the antenna array. However, if the width $W_E$ is too large, the front-to-back ratio and endfire gain of the antenna array might be bad. When the radiating elements are periodically placed along the parallel strip line, the periodicity might introduce high-order space harmonics, which could be graphically illustrated based on (1) [5]. Equation (1) corresponds to the array factor of a uniform array. To simplify the analysis, the element number $N$ is selected as 37 and the wavenumber $k$ is chosen as $k_0$. The beam directions of the different space harmonics could be calculated by (2) [27]. As shown in Fig. 5, when the radiating element separation $P$ is larger than 0.5 wavelength, the $n = -1$ space harmonic begins to coexist with the fundamental ($n = 0$) space harmonic. By increasing the period $P$, the beam related to the $n = -1$ space harmonic swings up from backward endfire toward broadside. Thereby, as a compromise, the $W_E = 8$ mm and period $P = 10$ mm are adopted by the antenna array to achieve a solely fundamental space harmonic over the entire operating band from 4 to 10.5 GHz.

To constrain the electric field concentrating in the parallel strip line to reduce the undesired radiating, the height $H$ should be small. Besides, for the parallel strip line itself, it should obtain a good match alone. Hence, as exhibited in Table I, the height $H = 2$ mm, which is 0.087 wavelength at the highest operating

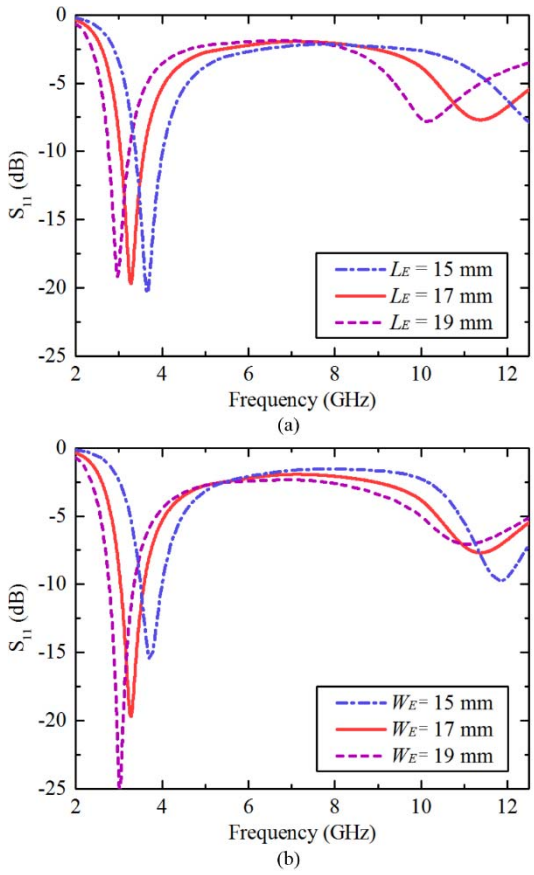


Fig. 4. Reflection magnitudes of the radiating elements with different (a) lengths $L_E$ or (b) widths $W_E$.

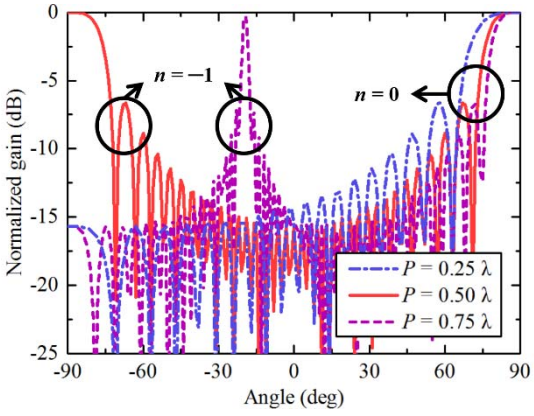


Fig. 5. Normalized array factors with different periods $P$, where $+y$-axis is corresponding to $+90°$.

frequency point of 10.5 GHz, and the width $W$ is optimized as 10 mm. The performance of the parallel strip line is illustrated in Fig. 6. The reflection magnitude is lower than $-14.5$ dB and the transmission magnitude is higher than $-1.15$ dB from 4 to 10.5 GHz. After adding the radiating elements on the parallel strip line, the normalized phase constant of the antenna array versus frequency is exhibited in Fig. 7. For a comparison, the phase constants in free space, of the theoretical Hansen–Woodyard (H-W) condition [28], and on the antenna array are shown together. By utilizing the air-substrate parallel strip line as the feed structure,

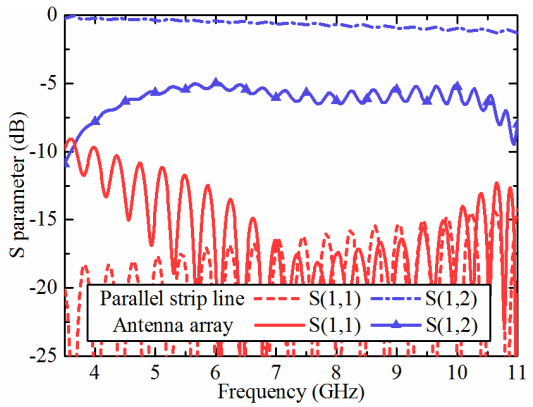


Fig. 6. S-parameters of the parallel strip line with or without the radiating elements.

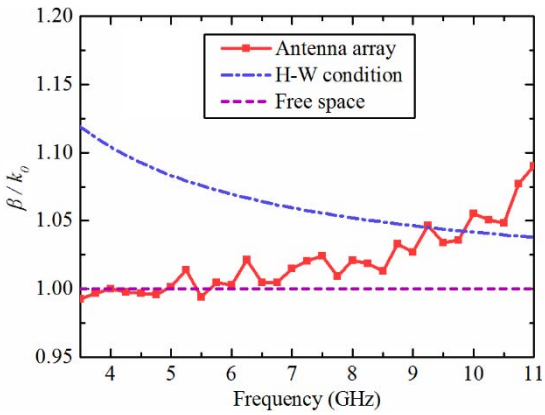


Fig. 7. Normalized phase constant versus frequency.

the fundamental space harmonic of the antenna array is TEM mode. Because of the addition of the radiating elements, the phase constant $\beta$ of the antenna array is perturbed somewhat in value. However, the phase constant of the antenna array is still stable versus frequency and moderate for the endfire radiation. Besides, according to the solution in [26], a slightly large phase constant could improve the directivity.

As depicted in Fig. 6, compared with the parallel strip line alone, most of the portion of the array's reflection magnitude remains lower than $-10$ dB, whereas the transmission magnitude of the antenna array drops significantly due to the coupling of the radiating element. Because the radiating elements do not dramatically influence the match of the parallel strip line, the two parts could be designed and optimized independently.

## III. Experimental Results

The fabricated prototype of the antenna array is presented in Fig. 8. It is made using two 0.5 mm thick copper plates and two SMA connectors. In the assembly, a 2 mm thick foam is used as a support in the parallel strip line. The antenna array and the foam are taped firmly together. In the measured setup, Port 1 is fed and Port 2 is connected with a matching load. The vector network analyzer (N9917A, 45 MHz–18 GHz) is adopted to measure the S-parameters, and a far-field anechoic chamber is employed to measure the gain and radiation pattern.

As illustrated in Fig. 9, the simulated reflection magnitude is lower than $-10$ dB from 4 to 11 GHz, and the measured reflection

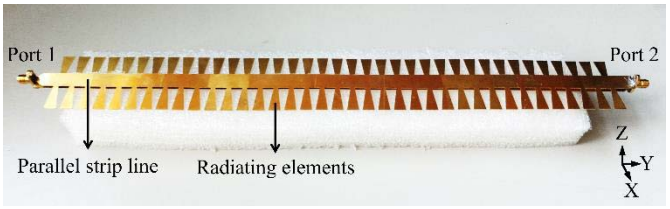


Fig. 8. Prototype of the antenna array.

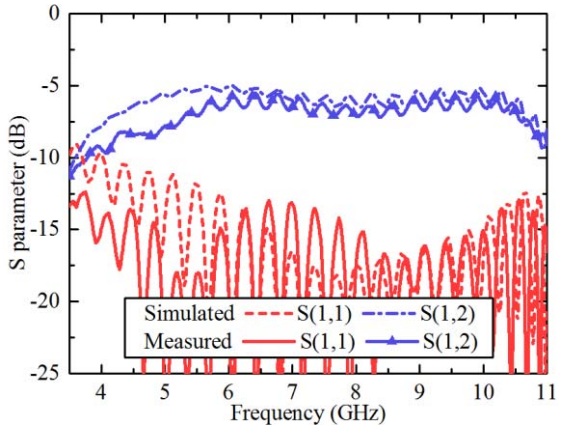


Fig. 9. Simulated and measured S-parameters of the antenna array.

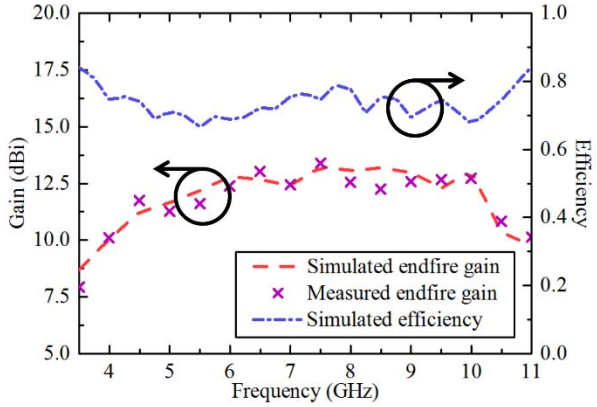


Fig. 10. Simulated and measured endfire gains, and simulated radiation efficiency of the antenna array.

magnitude is lower than −10 dB from the 3.5 to 11 GHz. Since the energy in the parallel strip line is effectively coupled by the radiating elements, from −3.5 to 11 GHz, the simulated transmission coefficient is lower than −5 dB, and the measured transmission coefficient is lower than −5.5 dB. The endfire gain and the efficiency of the antenna array are depicted in Fig. 10. It is found that the simulated and measured gains are relatively stable, which are higher than 10.1 dBi over the entire operating bandwidth from 4 to 10.5 GHz. The simulated maximum gain is 13.3 dBi at the frequency of 8.25 GHz, and the measured maximum gain 13.5 dBi at the frequency of 7.5 GHz. The simulated −1 and −3 dB gain bandwidths of the antenna array are 58.6% and 89.7%, respectively. The measured −1 and −3 dB gain bandwidths of the antenna array are 55.2% and 81.4%, respectively. Similar to the typical leaky-wave antenna arrays [19], [20], [29], the coupling between the radiating elements and parallel strip line is adjusted to a low level

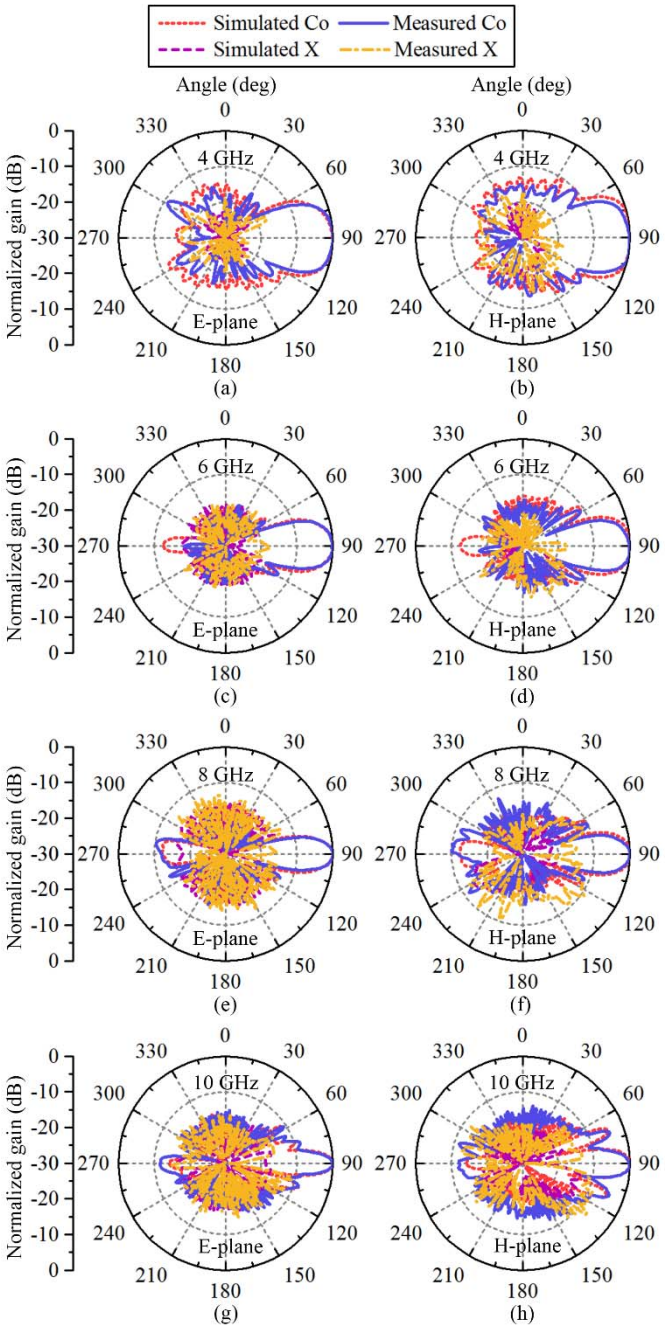


Fig. 11. Simulated and measured normalized radiation patterns on E-plane (*yoz* plane) and H-plane (*xoy* plane) at the frequencies of (a) and (b) 4 GHz, (c) and (d) 6 GHz, (e) and (f) 8 GHz, and (g) and (h) 10 GHz.

to improve the magnitude distribution on the radiating aperture [25], [26]. Furthermore, the loading influence of the radiating elements on the parallel strip line decreases, which is good for realizing a broad operating bandwidth. However, due to the low coupling level, more energy is absorbed by Port 2, leading to total efficiency reduction. Because the antenna array is designed and fabricated with an all-metal structure, the total efficiency is approximately calculated by

$$\text{Total efficiency} = 1 - |S_{11}|^2 - |S_{12}|^2. \tag{3}$$

As shown in Fig. 10, the simulated total efficiency of the antenna array varies from 0.67 to 0.84 over the operating bandwidth.

TABLE II
COMPARISON OF THE BANDWIDTH AND THE ENDFIRE GAIN

| Ref. | Type | $f_0$ (GHz) | $\varepsilon_r$ | Length ($\lambda_0$) | Width ($\lambda_0$) | Front-to-back ratio (dB) | Bandwidth (%) | Min. gain (dBi) | Max. gain (dBi) |
|---|---|---|---|---|---|---|---|---|---|
| [7] | Quasi-Yagi | 29.0 | 2.20 | 1.26 | 0.72 | 5.5 | 74.0 [$S_{11}$ < -9 dB] | 4.0 | 8.0 |
| [8] | Quasi-Yagi | 7.05 | 4.40 | 0.82 | 0.85 | 15 | 92.2 | 4.1 | 7.0 |
| [9] | Quasi-Yagi | 7.60 | 4.40 | 0.86 | 0.76 | 20 | 105.3 | 4.1 | 6.8 |
| [10] | Quasi-Yagi | 4.90 | 10.2 | 1.36 | 0.98 | 15 | 40.8 | 6.5 | 8.0 |
| [15] | Log-periodic | 7.40 | 2.33 | 6.49 | 0.97 | 25 | 86.5 | 4.4 | 9.9 |
| [16] | Log-periodic | 33.5 | 2.20 | 1.65 | 1.94 | 20 | 38.8 | 7.5 | 11.1 |
| [17] | Log-periodic | 30.5 | 2.20 | 2.34 | 1.42 | 17 | 62.3 | 6.5 | 10.9 |
| [18] | Log-periodic | 45.0 | 2.20 | 2.66 | 1.50 | 25 | 22.2 | 7.3 | 12.5 |
| Ours | Leaky-wave | 7.25 | 1.00 | 9.18 | 1.02 | 18 | 89.7 | 10.1 | 13.5 |

The simulated and measured normalized radiation patterns of the antenna array on E-plane (*yoz* plane) and H-plane (*xoy* plane) are depicted in Fig. 11. To evaluate the radiation performance, the radiation patterns at 4, 6, 8, and 10 GHz are chosen for presentation. With the increase in the frequency, the effective radiating aperture length and the phase constant of the antenna array increase, leading to a narrower beamwidth and a higher sidelobe level [24]. Because of the small radiating element separation $P$ ($P \approx 0.35$ wavelength at the highest operating frequency of 10.5 GHz) and the moderate phase constant $\beta$, the antenna array has a good front-to-back ratio level. From Fig. 11, the simulated and measured cross-polarization discriminations are both higher than 16.5 dB on the endfire direction, and the simulated and measured front-to-back ratios are both higher than 11.5 dB. When the frequency point changes from 4 to 10 GHz, the simulated half-power beam widths (HPBWs) on E-plane and H-plane vary from 39° to 12° and from 47° to 14°, respectively, and the measured HPBWs on E-plane and H-plane vary from 38° to 11° and from 40° to 14°, respectively. The slight difference between the simulated and measured results might be attributed to the fabrication and assembly errors. However, they are still in good agreement.

The comparison of the dimensions and performances between the proposed antenna array and the antennas for the same purpose in the open literature is presented in Table II, where *front-to-back ratio* is achieved at the center frequency $f_0$, and $\varepsilon_r$ is the dielectric constant of the material filling in the antenna. From Table II, with a longer radiating aperture, the proposed antenna array has a higher gain than the other antennas. Moreover, because 1) the radiating elements obtain the energy from the parallel strip line with a stable coupling level; 2) the small period $P$ constrains the antenna array existing solely fundamental space harmonic; and 3) the air-substrate parallel strip line provides a moderate phase constant $\beta$ for the antenna array, the proposed antenna array achieves a broad operating bandwidth and a high front-to-back ratio as well.

## IV. CONCLUSION

In this communication, we focus our attention on realizing a planar endfire antenna for wideband and high-gain applications. By designing a large radiating aperture, adopting the air-substrate parallel strip line as the feed structure and optimizing the dimension of the radiating element, a novel antenna array with a simple and planar configuration is designed. It obtains a good match and a stable endfire radiation with a high front-to-back ratio over the operating bandwidth from 4 to 10.5 GHz. The endfire gain of the antenna array varies from 10.1 to 13.5 dBi. Since the antenna array could be fabricated by thin metallic plates, it attains the advantages of lightweight, low cost, and easy fabrication. Considering the merits mentioned above, the antenna array is a potential candidate for the broadband long-distance wireless applications with the demand of the endfire radiation.

## REFERENCES


[1] Z. Yang, L. Zhang, and T. Yang, "A microstrip magnetic dipole Yagi–Uda antenna employing vertical I-shaped resonators as parasitic elements," *IEEE Trans. Antennas Propag.*, vol. 66, no. 8, pp. 3910–3917, Aug. 2018.

[2] E. Guo, J. Liu, and Y. Long, "A mode-superposed microstrip patch antenna and its Yagi array with high front-to-back ratio," *IEEE Trans. Antennas Propag.*, vol. 65, no. 12, pp. 7328–7333, Dec. 2017.

[3] W. Zhou, J. Liu, and Y. Long, "A broadband and high-gain planar complementary Yagi array antenna with circular polarization," *IEEE Trans. Antennas Propag.*, vol. 65, no. 3, pp. 1446–1451, Mar. 2017.

[4] J. Liu and Q. Xue, "Microstrip magnetic dipole Yagi array antenna with endfire radiation and vertical polarization," *IEEE Trans. Antennas Propag.*, vol. 61, no. 3, pp. 1140–1147, Mar. 2013.

[5] C. A. Balanis, *Antenna Theory Analysis and Design*, 3rd ed. Hoboken, NJ, USA: Wiley, 2005, p. 294, 577, and 623.

[6] A. Abbosh, "Ultra-wideband quasi-Yagi antenna using dual-resonant driver and integrated balun of stepped impedance coupled structure," *IEEE Trans. Antennas Propag.*, vol. 61, no. 7, pp. 3885–3888, Jul. 2013.

[7] H. Chu, Y.-X. Guo, H. Wong, and X. Shi, "Wideband self-complementary quasi-Yagi antenna for millimeter-wave systems," *IEEE Antennas Wireless Propag. Lett.*, vol. 10, pp. 322–325, 2011.

[8] J. Wu, Z. Zhao, Z. Nie, and Q.-H. Liu, "Design of a wideband planar printed quasi-Yagi antenna using stepped connection structure," *IEEE Trans. Antennas Propag.*, vol. 62, no. 6, pp. 3431–3435, Jun. 2014.

[9] J. Wu, Z. Zhao, Z. Nie, and Q.-H. Liu, "Bandwidth enhancement of a planar printed quasi-Yagi antenna with size reduction," *IEEE Trans. Antennas Propag.*, vol. 62, no. 1, pp. 463–467, Jan. 2014.

[10] K. Han, Y. Park, H. Choo, and I. Park, "Broadband CPS-fed Yagi-Uda antenna," *Electron. Lett.*, vol. 45, no. 24, pp. 1207–1209, Nov. 2009.

[11] X. Gao, Z. Shen, and C. Hua, "Conformal VHF log-periodic balloon antenna," *IEEE Trans. Antennas Propag.*, vol. 63, no. 6, pp. 2756–2761, Jun. 2015.

[12] Z. Hu, Z. Shen, W. Wu, and J. Lu, "Low-profile log-periodic monopole array," *IEEE Trans. Antennas Propag.*, vol. 63, no. 12, pp. 5484–5491, Dec. 2015.

[13] Q. Song, Z. Shen, and J. Lu, "Log-periodic monopole array with uniform spacing and uniform height," *IEEE Trans. Antennas Propag.*, vol. 66, no. 9, pp. 4687–4694, Sep. 2018.

[14] Q. Chen, Z. Hu, Z. Shen, and W. Wu, "2–18 GHz conformal low-profile log-periodic array on a cylindrical conductor," *IEEE Trans. Antennas Propag.*, vol. 65, no. 2, pp. 729–736, Feb. 2018.

[15] F. Merli, J.-F. Zurcher, A. Freni, and A. K. Skrivervik, "Analysis-design and realization of a novel directive ultra-wideband antenna," *IEEE Trans. Antennas Propag.*, vol. 57, no. 11, pp. 3458–3466, Nov. 2009.

[16] G. Zhai, Y. Cheng, Q. Yin, L. Chiu, S. Zhu, and J. Gao, "Super high gain substrate integrated clamped-mode printed log-periodic dipole array antenna," *IEEE Trans. Antennas Propag.*, vol. 61, no. 6, pp. 3009–3016, Jun. 2013.

[17] G. Zhai, Y. Cheng, Q. Yin, S. Zhu, and J. Gao, "Gain enhancement of printed log-periodic dipole array antenna using director cell," *IEEE Trans. Antennas Propag.*, vol. 62, no. 11, pp. 5915–5919, Nov. 2014.

[18] Q.-X. Chu, X.-R. Li, and M. Ye, "High-gain printed log-periodic dipole array antenna with parasitic cell for 5G communication," *IEEE Trans. Antennas Propag.*, vol. 65, no. 12, pp. 6338–6344, Dec. 2017.

[19] J. Liu, D. R. Jackson, and Y. Long, "Substrate integrated waveguide (SIW) leaky-wave antenna with transverse slots," *IEEE Trans. Antennas Propag.*, vol. 60, no. 1, pp. 20–29, Jan. 2012.

[20] J. Liu, D. R. Jackson, Y. Li, C. Zhang, and Y. Long, "Investigations of SIW leaky-wave antenna for endfire-radiation with narrow beam and sidelobe suppression," *IEEE Trans. Antennas Propag.*, vol. 62, no. 9, pp. 4489–4497, Sep. 2014.

[21] P. Liu, H. Feng, Y. Li, and Z. Zhang, "Low-profile endfire leaky-wave antenna with air media," *IEEE Trans. Antennas Propag.*, vol. 66, no. 3, pp. 1086–1092, Mar. 2018.

[22] Y. Hou, Y. Li, Z. Zhang, and Z. Feng, "Narrow-width periodic leaky-wave antenna array for endfire radiation based on Hansen–Woodyard condition," *IEEE Trans. Antennas Propag.*, vol. 66, no. 11, pp. 6393–6396, Nov. 2018.

[23] Y. Hou, Y. Li, Z. Zhang, and M. F. Iskander, "Microstrip-fed surface-wave antenna for endfire radiation," *IEEE Trans. Antennas Propag.*, vol. 67, no. 1, pp. 580–584, Jan. 2019.

[24] Y. Hou, Y. Li, Z. Zhang, and M. F. Iskander, "All-metal endfire antenna with high gain and stable radiation pattern for the platform-embedded application," *IEEE Trans. Antennas Propag.*, vol. 67, no. 2, pp. 730–737, Feb. 2019.

[25] E. M. O'Connor, D. R. Jackson, and S. A. Long, "Extension of the Hansen–Woodyard condition for endfire leaky-wave antennas," *IEEE Antennas Wireless Propag. Lett.*, vol. 9, pp. 1201–1204, 2010.

[26] W. Fuscaldo, D. R. Jackson, and A. Galli, "Beamwidth properties of endfire 1-D leaky-wave antennas," *IEEE Trans. Antennas Propag.*, vol. 65, no. 11, pp. 6120–6125, Nov. 2017.

[27] J. L. Volakis, *Antenna Engineering Handbook*, 4th ed. New York, NY, USA: McGraw-Hill, 2007, pp. 11–13.

[28] W. W. Hansen and J. R. Woodyard, "A new principle in directional antenna design," *Proc. IRE*, vol. 26, no. 3, pp. 333–345, Mar. 1938.

[29] Y. Li, Z. Zhang, C. Deng, Z. Feng, and M. F. Iskander, "2-D planar scalable dual-polarized series-fed slot antenna array using single substrate," *IEEE Trans. Antennas Propag.*, vol. 62, no. 4, pp. 2280–2283, Apr. 2014.